

## Progress of plasma assessment in JT-60SA

T. Fujita<sup>1</sup> for the JT-60SA Team

<sup>1</sup>*JT-60SA Project Team, 801-1 Mukoyama, Naka, Ibarakai, 311-0193 Japan.*

### 1. Introduction

The construction and exploitation of the JT-60SA device will be conducted in Japan under the Satellite Tokamak Programme, to be undertaken as part of the Broader Approach agreement jointly implemented by Europe and Japan, and the Japanese National Programme. The mission of JT-60SA is to contribute to the early realization of fusion energy by supporting the exploitation of ITER and research towards DEMO by addressing key physics issues associated with these machines. JT-60SA shall: i) be capable of confining break-even equivalent class high-temperature deuterium plasmas at a plasma current  $I_p$  of  $\sim 5.5$  MA, a major radius of  $\sim 3$  m, and lasting for a duration longer than the timescales characteristic of plasma processes (flattop duration  $\sim 100$  s); ii) pursue full non-inductive steady-state operation with high plasma beta close to, and exceeding, the no-wall ideal stability limits; iii) establish ITER-relevant high density plasma regimes well above the H-mode power threshold.

In late 2007 the BA Parties, prompted by cost concerns, asked the JT-60SA Team to carry out a re-baselining effort with the purpose to fit in the original budget while aiming to retain the machine mission, performance, and experimental flexibility. Subsequently, along 2008, the JT-60SA Team has undertaken a machine re-optimisation, that led to a machine design with an aspect ratio of  $\sim 2.5$ , and that was followed by engineering design activities aimed to further reduce costs. This effort led the Parties to the approval of the new design in late 2008 [1]. In this paper, progress in the machine design is presented in section 2, and the assessment of plasma performance in the new design is presented in section 3.

### 2. Progress in the design

Consequences of re-designing from the previous design [2] include the following. (1) The toroidal field was reduced from  $\sim 2.68$  T to  $\sim 2.25$  T while the nominal plasma current was kept 5.5 MA with reduced plasma aspect ratio ( $A \sim 2.5$ ). (2) The number of Equilibrium Field (EF) coils was reduced from 7 to 6 keeping plasma shape flexibility. (3) A phased equipment plan was adopted for the heating and current drive systems and for the divertor.

Figure 1 shows comparison of elevation view of old and new superconducting magnet, vacuum vessel and in-vessel components. The radial thickness of toroidal field (TF) coils is significantly reduced due to reduced  $B_t$ , while the overall outboard and top/bottom size of the TF coils was kept so to allow the machine to be installed within the existing NBI alignment and envelopes. The vertical and inboard space obtained through the use of a slender TF coil has allowed a larger plasma elongation with a reduced TF ripple and an increased radius of central solenoid (CS) with a larger available flux swing. The maximum value of TF ripple in a

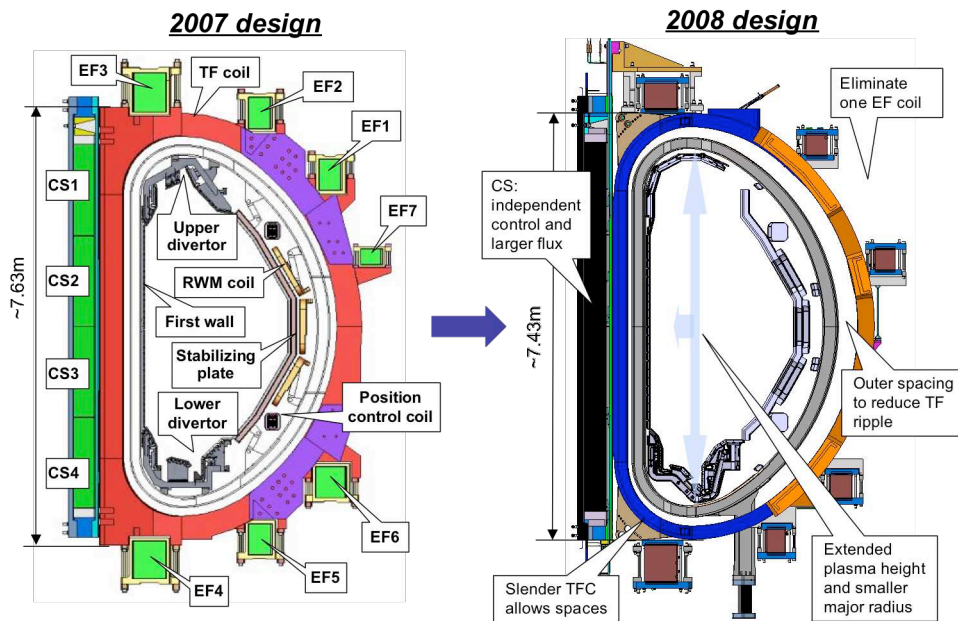


Figure 1. Comparison of elevation view of old and new designs.

full-bore plasma was reduced from 1.5% to 0.9% at the plasma outboard surface. This value would be reduced further to  $\sim 0.5\%$  by means of ferromagnetic inserts inside the vacuum vessel. In the poloidal field coil systems, the distribution of turns in 6 EF coils was optimized considering the most probable plasma configurations, while the currents in the two central CS modules have become controlled independently, which allowed expanding the operational space in  $(\beta_p, i_i)$  with the reduced total conductor length.

The design of lower divertor cassette, which will be installed from the beginning of tokamak operation, was optimized so as to obtain higher plasma triangularity ( $\delta_x \sim 0.5$ ) in a Lower Single Null (LSN) configuration, as shown in Figure 1. Vertical targets, with a V-shaped corner for the outer one, are employed as in the previous design [3]. At the initial phase of tokamak operation, a combination of bolted CFC targets for most of cassettes and monoblock CFC targets for a few cassettes will be used, while the former will be exchanged to the monoblock CFC targets in a later phase, in order to allow high heat flux (up to  $15 \text{ MW/m}^2$ ) operation lasting for 100 s. Use of tungsten coated CFC monoblock is a future option. All plasma-facing components including the divertor target, baffle plates and inner/outer first wall will be water-cooled at  $40^\circ \text{C}$ . The divertor cassettes shall be compatible with remote handling maintenance to allow long pulse high performance plasma operation with a large neutron yield. In the vacuum vessel, in addition, three sets of copper coils consisting of a pair of fast plasma position control coils, 18 error field correction coils and 18 RWM control coils will be installed.

With reduction of  $B_t$ , the frequency of ECRF has been changed from 140 GHz (4 MW)+110 GHz (3 MW) to 110 GHz (7 MW). This allows ECCD of 7 MW with the second harmonic X-mode down to 1.7 T, covering a range expected for high  $\beta_N$  steady-state operation, while on-axis heating in high-density plasmas will be limited due to the lower

Table 1. Operation phases and status of key components.

	Phase	Expected Duration		Annual Neutron Limit	Remote Handling	Divertor	P-NB	N-NB	ECRF	Max Power	Power x Time
Initial Research Phase	phase I	1-2 y	<b>H</b>	-	R&D	LSN partial monoblock	10MW	10MW	1.5MW x100s + 1.5MW x5s	23MW	NB: 20MW x 100s 30MW x 60s duty = 1/30  ECRF: 100s
	phase II	2-3y	<b>D</b>	4E19			Perp. 13MW		33MW		
Integrated Research Phase	phase I	2-3y	<b>D</b>	4E20	Use	LSN full-monoblock	Tang. 7MW	7MW	37MW		
	phase II	>2y	<b>D</b>	1E21			41MW		41MW x 100s		
Extended Research Phase		>5y	<b>D</b>	1.5E21		DN	24MW				

cut-off density ( $7.5 \times 10^{19} \text{ m}^{-3}$ ).

The JT-60SA device will be upgraded step by step according to a phased operation plan consisting of i) an initial research phase (hydrogen phase and deuterium phase), ii) an integrated research phase, and iii) an extended research phase as shown in Table 1. A JT-60SA research plan is under development, in which a staged approach will be employed consistently with the phased upgrade in machine capability.

### 3. Plasma performance assessment

The plasma performance expected in the newly designed JT-60SA was assessed and compared with the assessment for the previous design [3]. The results are shown below, which show all the scientific missions can be achieved as before.

For shape controllability, typical LSN and DN configurations are shown in Figure 2; A is around 2.5 and  $q_{95}$  is close to 3 owing to reduced A in spite of lowered  $B_t$  in both configurations, while  $\kappa_x \sim 1.8$  (1.9),  $\delta_x \sim 0.49$  (0.60) and  $S \sim 5.7$  (6.2) for LSN (DN), where S is the shape factor defined by  $S = q_{95} I_p [\text{MA}] / a [\text{m}] B_t [\text{T}]$ .

For break-even class plasma with long duration, similar  $n\tau T$ ,  $(5-7) \times 10^{20} \text{ m}^{-3} \cdot \text{s} \cdot \text{keV}$  with  $I_p = 5.5 \text{ MA}$ ,  $f_{GW} = 0.8$  and  $HH_{98y2} = 1.1-1.3$ , is expected with a longer duration due to the increased available Volt-seconds, where  $f_{GW}$  is the ratio of average density to the Greenwald density. In these plasmas, the density at  $f_{GW} = 0.8$  is  $1 \times 10^{20} \text{ m}^{-3}$ , namely ITER-relevant, while the threshold power for L to H transition ( $P_{LtoH}$ ) is 15 MW.

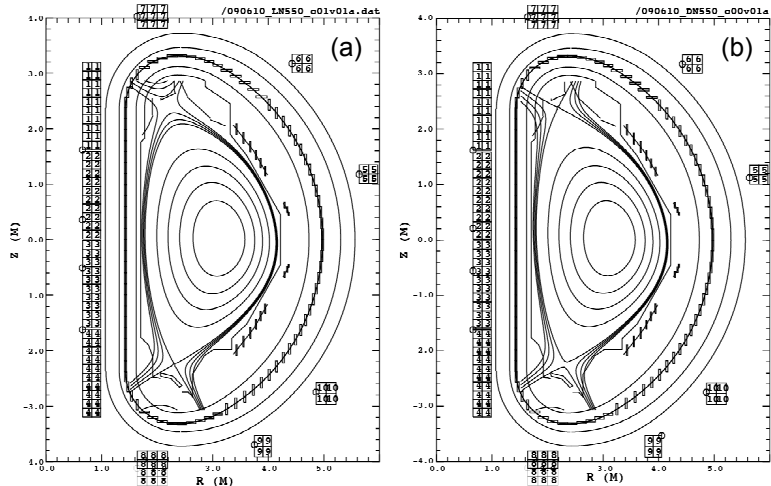


Figure 2. Examples of plasma configurations with  $I_p = 5.5 \text{ MA}$ . (a) Lower single null. (b) Double null.

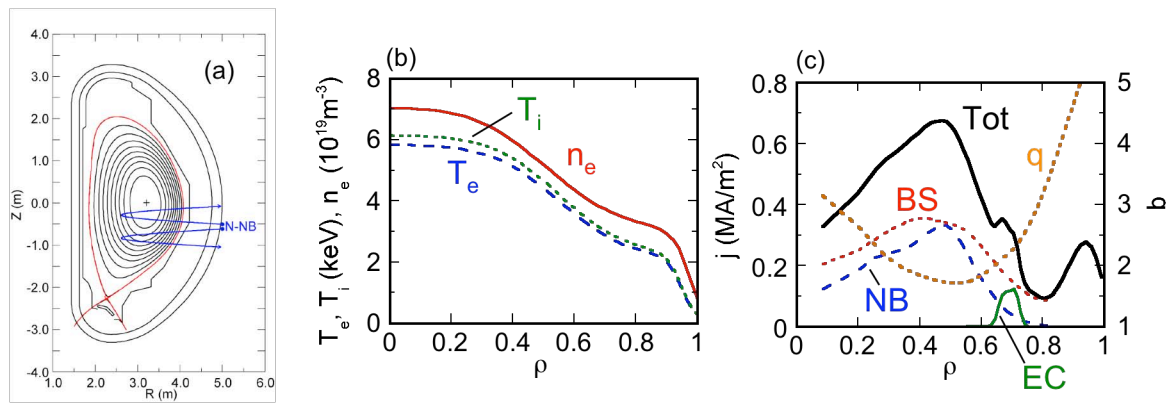


Figure 3. (a) Configuration, (b)  $n_e$ ,  $T_e$ , and  $T_i$  profiles and (c)  $j$  and  $q$  profiles in a full CD plasma.

Hence with 30 MW heating,  $P_{\text{heat}}/P_{\text{LtoH}}$  reaches 2 and good confinement is expected.

For non-inductive steady-state operation, high  $\beta_N$  plasmas are expected to be fully non-inductively driven with slightly reduced  $I_p$  and/or  $\beta_N$  compared to those expected in the previous design. Figure 3 that shows an example with  $I_p = 2.3$  MA,  $B_t = 1.7$  T,  $q_{95} = 5.6$ ,  $f_{\text{GW}} = 0.85$ ,  $f_{\text{BS}} = 0.67$ ,  $\beta_N = 4.1$ ,  $\text{HH}_{98y2} = 1.3$ ,  $P_{\text{heat}} = 37$  MW (20 MW of N-NB, 10 MW of P-NB and 7 MW of ECRF). Here  $f_{\text{BS}}$  is the fraction of the bootstrap current in the total plasma current. Profiles of the inductive, bootstrap, beam-driven, and ECRF-driven currents are calculated with the ACCOME code using assumed  $n_e$ ,  $T_e$  and  $T_i$  profiles. The beam driven current has its peak around  $r/a \sim 0.5$  due to the downward shifted N-NBI. The resultant  $q$  profile has a reversed shear configuration with  $q_{\text{min}} \sim 1.7$  at  $r/a \sim 0.5$ . For a reduced value of  $f_{\text{GW}}$  (0.6), a higher  $I_p$  of 2.9 MA would be non-inductively driven with the same  $\text{HH}_{98y2}$  of 1.3.

The divertor performance was simulated by using the SONIC code [4] for the newly designed lower divertor. The peak heat load  $q_{\text{peak}}$  will be maintained less than  $11 \text{ MW/m}^2$  by gas puffing ( $1.5 \times 10^{22} \text{ s}^{-1}$  or  $30 \text{ Pam}^3/\text{s}$ ) for the maximum heating power of 41 MW, 4MW of which is assumed to be radiated in the main plasma core, as shown in Figure 4. As impurity, a uniform fraction (2%) of carbon is assumed. The power radiated in the main plasma edge and in the SOL/divertor region is 23 MW. The main plasma density at the separatrix  $n_e^{\text{sep}}$  is  $2.8 \times 10^{19} \text{ m}^{-3}$ , which is acceptable in a 5.5MA operation. A lower  $n_e^{\text{sep}}$  of  $1.7 \times 10^{19} \text{ m}^{-3}$  ( $q_{\text{peak}} = 8.6 \text{ MW/m}^2$ ), compatible with lower  $I_p$  plasmas, is obtained with impurity seeding in the divertor region.

## References

- [1] S. Ishida et al., "Progress of the JT-60SA project", in the ITER session, this conference.
- [2] N. Hosogane et al, Fusion Sci. Tech. **52**, 375 (2007).
- [3] T. Fujita et al., Nucl. Fusion **47**, 1512 (2007).
- [4] K. Shimizu et al, Contrib. Plasma Phys. **48**, 270 (2008).

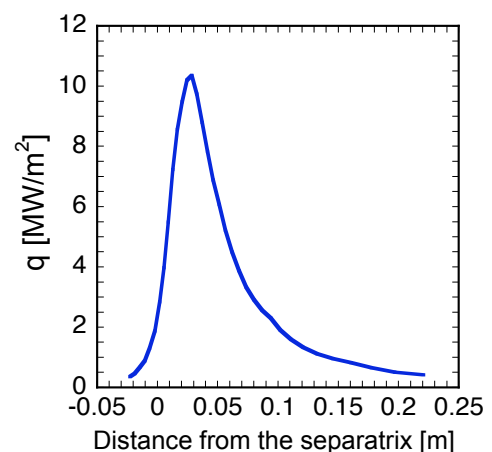


Figure 4. Heat flux density along the outer target.